Static Inhomogeneities in Thermoreversible Physical Gels

Fumiyoshi Ikkai and Mitsuhiro Shibayama

Department of Polymer Science and Engineering, Kyoto Institute of Technology, Matsugasaki, Sakyo-ku, Kyoto 606-8585, Japan
(Received 11 January 1999)

Thermoreversible gels of poly(vinyl alcohol)/Congo red in aqueous solutions have been studied by dynamic light scattering. Below T_{gel} ($\approx 43\,°C$), a speckle pattern appeared, while it disappeared for $T > T_{gel}$. This indicates that nonergodicity observed in chemically cross-linked gels also exists in thermoreversible physical gels. Analogous to the β and α relaxations of glasses, the intensity correlation function showed a power-law behavior for $T \leq T_{gel}$ and a stretched exponential behavior for $T \geq T_{gel}$, respectively, while the thermal fluctuations characteristic of polymer gels were present independent of T_{gel}. [S0031-9007(99)09308-4]

PACS numbers: 82.70.Gg, 61.43.Fs

Nonergodic media, such as glasses and gels, have frozen spatial inhomogeneities due to a frozen structure (in glasses) or topological constraints, i.e., cross-linking (in gels) [1]. One of the clear manifestations of nonergodicity is the appearance of speckles, i.e., random fluctuations in the scattered intensity as a function of sample position. Different from glasses, gels have another component of concentration fluctuations, i.e., thermal fluctuations [2–4]. Hence, the scattering from gels originates from the spatial inhomogeneities and thermal concentration fluctuations. It has generally been believed that the spatial inhomogeneities are characteristic features of chemical gels, and that it is hardly possible that one observes the speckles in physical gels. This stems from the presupposition that, in contrast to the chemically cross-linked gels for which the spatial inhomogeneities are instantaneously introduced during polymerization and/or cross-linking processes, the thermoreversible nature of cross-linking process prevents physical gels from acquiring an inhomogeneous distribution of cross-links, the resultant distribution of cross-links corresponding to the random conformation of network energy minima. However, it should be remarked that according to the linear elasticity theory of deformed networks due to cross-linking [5,6], the presence of speckles in physical gels is not unexpected.

In this Letter, we report the first observation of thermoreversible speckle appearance/annihilation in physical gels. Then, we discuss that the gelation threshold for physical gels can be characterized as (a) an appearance of a speckle pattern and (b) a power law behavior of the intensity correlation function (ICF). We specifically pay attention to the similarity and dissimilarity between gels and glasses and aim to extract the universality of sol-gel transitions. Poly(vinyl alcohol)/Congo red (PVA/CR) gels in aqueous solutions were chosen in this work because of the following reasons: (1) The gelation is governed by chemical equilibrium and hence the rate is quick enough (a few minutes) without hysteresis, (2) the sol-gel transition temperature, T_{gel}, is located at a temperature of easy handling, i.e., ~43 °C, and (3) the

sol-gel phase diagram [7], the microscopic structure [8], and (4) the enthalpy of gel melting are well characterized.

PVA (the degree of polymerization and the degree of saponification being 1800 and 99.96 mol%, respectively) was dissolved in boiling distilled water and filtered with a 0.2 μm filter. Aqueous solution of reagent grade Congo red (CR; $C_{32}H_{22}N_6Na_2O_6S_2$), a synthetic dye, was added to the PVA solution. The concentrations of PVA and CR were 680 and 10 mM, respectively. CR plays as a cross-linker of PVA via hydrogen bonding between -NH_2 group of CR and -OH group of PVA. The sol-gel transition temperature was determined to be $T_{gel} \approx 43\,°C$ by flow measurement. The details of the experiment and the sol-gel phase diagram are reported elsewhere [7]. Static and dynamic (SLS and DLS) light scattering experiments were carried out on PVA/CR gels in 10-mm-diameter test tube using a DLS/SLS-5000 (ALV, Co. Ltd., Langen, Germany) coupled with a 22 mW He-Ne laser (the wavelength being 632.8 nm), a static/dynamic enhancer, and an avalanche-photo-diode detector system, which allowed obtaining the coherence factor of 0.98.

Figure 1 shows the time average scattered intensity, $\langle I \rangle_T$, obtained at the scattering angle of 90° as a function of the sample position. The sample position was arbitrarily chosen by rotating the sample test tube. $\langle I \rangle_T$ at 20 °C fluctuates randomly with respect to the sample position and a speckle pattern appears. The amplitude of $\langle I \rangle_T$ in the speckle pattern decreased with increasing temperature, T, as shown in the cases of (b) $T = 38$, (c) 43, and finally disappeared at (d) 57 °C. The appearance and annihilation of the speckles were thermoreversible. The horizontal solid line indicates the ensemble average $\langle I \rangle_E$, obtained by taking ensemble average of $\langle I \rangle_T$, which merges into the dynamic component of the scattered intensity indicated by the dashed line, $\langle I_F \rangle_T$, at 57 °C. The method of the estimation of $\langle I_F \rangle_T$ is described later.

The time-average intensity time correlation function (ICF), $S_T(q, \tau)$, is defined by

$$S_T(q, \tau) = \langle I(q,0)I(q,\tau)\rangle_T / \langle I(q,0)\rangle_T^2 - 1, \quad (1)$$

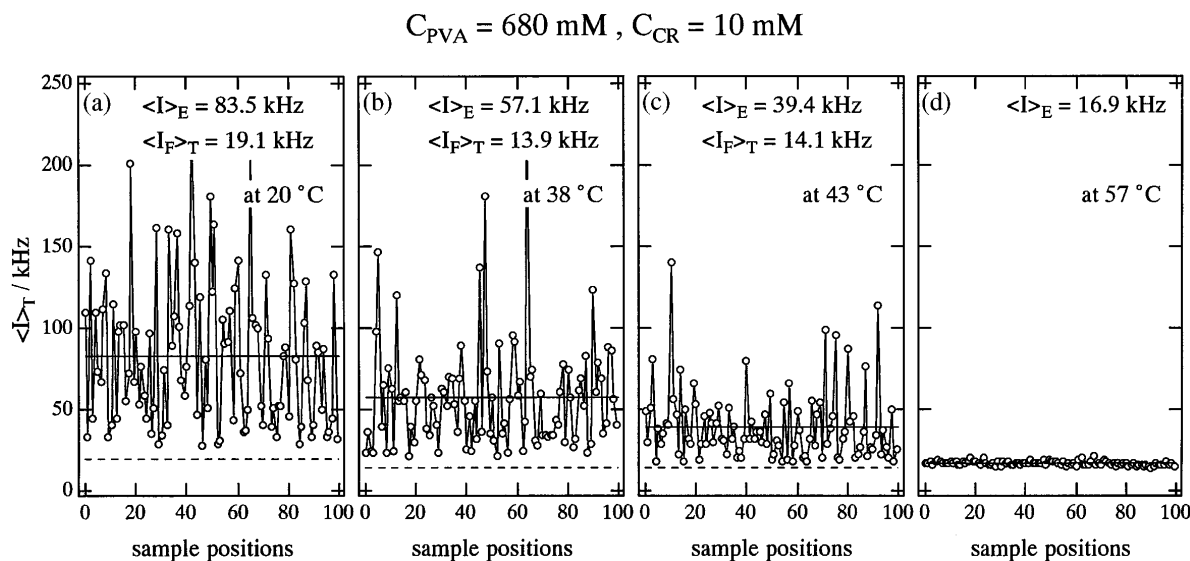$$C_{PVA} = 680 \text{ mM} , C_{CR} = 10 \text{ mM}$$

FIG. 1. Temperature dependence of the speckle patterns; (a) 20, (b) 38, (c) 43, and (d) 57 °C. The horizontal solid line and the dashed line indicate the ensemble average of the scattered intensity, $\langle I \rangle_E$, and the fluctuating component of the scattered intensity, $\langle I_F \rangle_T$, respectively.

where q is the scattering vector and τ is the time lag between two measurements of photon counting. The angular bracket with subscript T means time averaging. Figure 2 shows ICFs for PVA-CR gels ($T \leq 43$ °C) and sols ($T > 43$ °C), which shows a drastic change in the ICFs across 43 °C. Note that each ICF except for that of $T = 20$ °C was shifted vertically by 1 order of magnitude in order to avoid overlap. ICFs were sample position dependent for $T \leq 43$ °C and $S_T(q, \tau = 0)$ varies

dependent on the sample position due to nonergodicity. The solid lines in the figures are drawn with a power-law function [$T \leq 43$ °C; Eq. (2)] and with a stretched-exponential function [$T > 43$ °C; Eq. (3)], respectively,

$$S_T(q, \tau) \sim [1 + (\tau/\tau^*)]^{-(1-u)} \quad \text{(for gels)}, \quad (2)$$

$$S_T(q, \tau) \sim \exp[-(\tau/\tau_c)^{\beta}] \quad \text{(for sols and } \tau \geq \tau_c). \quad (3)$$

The τ^* is a characteristic time where the power-law behavior appears and u is the fractal dimension of the scattered photons [9]. The τ_c is another characteristic time related to the extent of spatial correlation and β is the stretched exponent. The exponent, u, was evaluated to be around 0.4 irrespective of temperatures and sample positions as far as the system was in the gel state. It should be noted that the power-law behavior was observed not only at the gelation threshold (near 43 °C) but also for gels ($T < T_{gel}$). A similar behavior in $S_T(q, \tau)$ was also observed in gelatin gels [10,11]. Ren et al. [11] discussed the analogy of these two types of relaxations, i.e., the stretched exponential and power law types, with the α and β relaxations of glasses. According to their results, u for gels is q dependent while that for glasses is not. Our result, however, shows that u is independent of q at least in the q range of from $0.01 < q < 0.025$ nm^{-1}. The independence of u with respect to q, observed in this work, is more reasonable since it is related to the size-independent relaxation [12]. In the case of chemical gels, Martin et al. observed a power-law behavior in poly(tetramethoxysilane) (PTMOS) gels with $u \approx 0.73$ at and above the gelation threshold [9]. The relatively large value of u and the power-law behavior in the gel state observed by Martin et al. may be ascribed to their high cross-link density which leads to glassification as
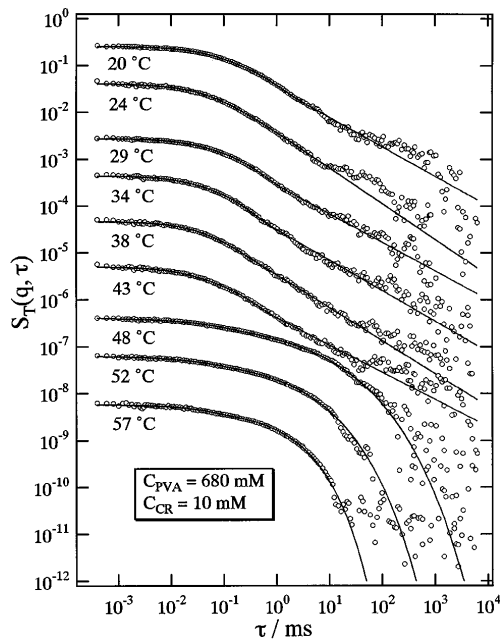

FIG. 2. Time intensity correlation function of PVA and CR aqueous systems at different temperatures. The solid lines are the results of curve fitting with a power-law function [Eq. (2)] and with a stretched exponential function [Eq. (3)].

well. On the other hand, for PTMOS gels with a lower cross-link density, a power-law behavior was exclusively observed only at the gelation threshold [13]. This means that the power-law behavior seems to be characteristic to glasses below the glass transition temperature where a β relaxation appears [14] and to the gels at least on the gelation threshold where the cluster distribution becomes a fractal [15,16].

Although the asymptotic forms of the ICF for the PVA/CR complex are described either by a stretched exponential function or a power-law function, a diffusive mode is always observed in gels at small τ region because of the Brownian motion of polymer chains. For a chemically cross-linked gel, it is reported that $S_T(q, \tau)$ is given by a single exponential function called *gel mode* [17],

$$S_T(q, \tau) = A \exp[-2D_A q^2 \tau], \tag{4}$$

where D_A is the apparent diffusion coefficient and A ($0 < A \le 1$) is the initial amplitude of ICF. In the case of a nonergodic medium like a gel [4,18], D_A scatters randomly with sample position in the range of $D/2 < D_A < D$, where D is the collective diffusion coefficient of the system. More precisely, $S_T(q, \tau)$ is given by [1,19,20]

$$S_T(q, \tau) = X^2 \exp(-2Dq^2\tau)$$
$$+ 2X(1 - X) \exp(-Dq^2\tau). \tag{5}$$

The variable X ($\equiv \langle I_F \rangle_T / \langle I \rangle_T$) denotes the ratio of the intensity from thermal fluctuations to that from total intensity at a given sample position. The fluctuating component in the scattered intensity, $\langle I_F \rangle_T$, can be extracted by plotting D_A vs $\langle I \rangle_T$ [19] or $\langle I \rangle_T / D_A$ vs $\langle I \rangle_T$, i.e., [21,22]

$$\frac{\langle I \rangle_T}{D_A} = \frac{2}{D} \langle I \rangle_T - \frac{\langle I_F \rangle_T}{D}. \tag{6}$$

The exponential-type functions for $S_T(q, \tau)$ seem to be valid for chemical gels, such as poly(acrylamide) and

homologues [22,23]. Although $S_T(q, \tau)$ for physical gels has a long-relaxation tail as shown above, we assume that $S_T(q, \tau)$ for the small-τ range ($\tau \ll \tau^*$ or $\tau \ll \tau_c$), is also given by Eq. (5) and apply the same analysis conducted for chemical gels to physical gels. Figure 3 shows the decomposition plot from which $\langle I_F \rangle_T$ and D are evaluated. D_A is estimated by the initial slope of $S_T(q, \tau)$, i.e., $D_A = -(1/2q^2)\partial \ln S_T(q, \tau)/\partial \tau|_{\tau=0}$. At 20 °C, the data points fall on a straight line given by Eq. (6). Note that the range of $\langle I \rangle_T$ decreases with increasing T. At 57 °C, all the data points collapse at a single point. This indicates that the system becomes an ergodic medium, i.e., a polymer solution. The time fluctuating component, $\langle I_F \rangle_T$, shown by the dashed lines in Fig. 1, was thus obtained.

Temperature variations of $\langle I \rangle_E$, $\langle I_F \rangle_T$, D, and the correlation length ξ ($\approx kT/6\pi\eta D$) are shown in Fig. 4, where η is the solvent viscosity and kT is the Boltzmann energy. The arrows in the figure indicate T_{gel} obtained by a flow test. $\langle I \rangle_E$ is a decreasing function of T. On the other hand, $\langle I_F \rangle_T$ seems to be T independent. Note that the variations of $\langle I \rangle_E$ and $\langle I_F \rangle_T$ were confirmed to be thermoreversible and $\langle I \rangle_E$ becomes equal to $\langle I_F \rangle_T$ for $T > T_{gel}$. The gradual decrease in $\langle I \rangle_E$ near T_{gel} indicates that the gel inhomogeneities are suppressed progressively by increasing T due to gel melting. The jump-wise change in D (and ξ) at $T \approx T_{gel}$ is quite interesting. This suggests that the spatial correlation is longer in the sol state than in the gel state. In other words, the spatial correlation is screened by cross-links in the gel state. It is noteworthy that such a kind of discrete change in ξ was not observed in chemical gels [22].

The nontrivial contribution of the thermal fluctuating component in the scattered intensity and the diffusive mode in the dynamics may be one of the characteristic features of gels. An analogy between sol/gel and glasses is seen particularly in the slow dynamics, e.g., for the
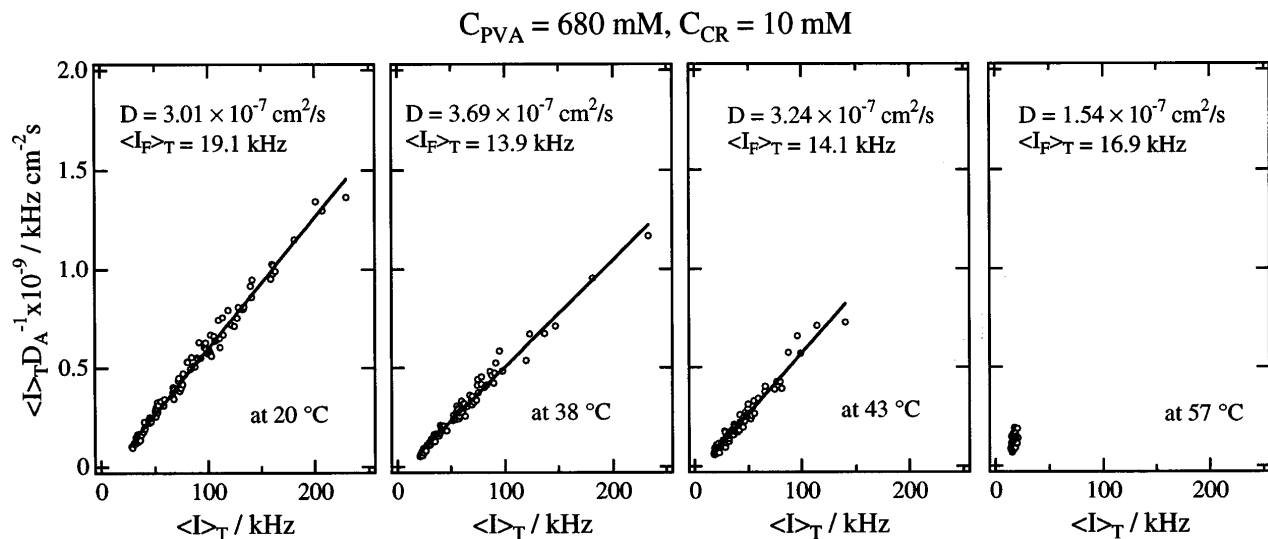
$$C_{PVA} = 680 \text{ mM}, \quad C_{CR} = 10 \text{ mM}$$

FIG. 3. $\langle I \rangle_T / D_A$ vs $\langle I \rangle_T$ plots for PVA and CR at different temperatures. The values of D and $\langle I_F \rangle_T$ are estimated from the slope and intercept, respectively.
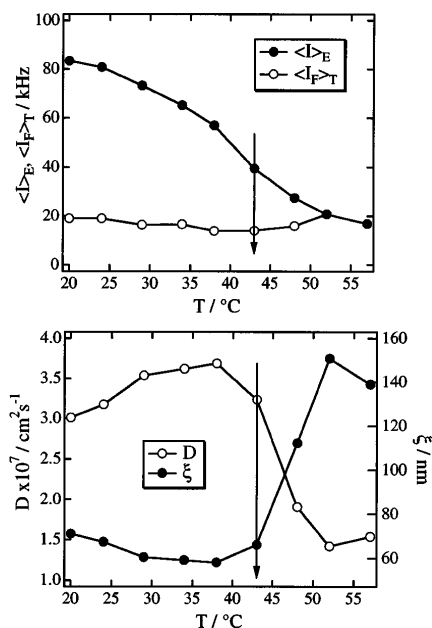
FIG. 4.   Temperature dependence of $\langle I \rangle_E$, $\langle I_F \rangle_T$, D, and ξ. The arrow indicates the sol-gel transition temperature.

regime of $\tau \gg \tau^*$. In the sol regime, ICF is described by a stretched exponential function, which corresponds to the α relaxation of glasses. In this case, both sols and glasses above the critical temperature (about 1.2 times higher than the glass transition temperature [24]) are ergodic media. At the gelation threshold, ICF becomes a power-law function, indicating a formation of fractallike hierarchical structure and suppression of translational diffusion of clusters. The β relaxation of glasses, on the other hand, is dominated by frozen structure. A similar situation may be attained in a gel when it is glassified by a high density cross-linking as is observed in silica gels. The PVA/CR gels may belong to this class. Gels with a low cross-link density, e.g., slightly cross-linked chemical gels, on the other hand, preserve a fast diffusive mode with a negligible contribution of the slow mode [23].

Static inhomogeneities and the dynamics of thermo-reversible physical gels comprising poly(vinyl alcohol) and Congo red (PVA/CR) have been investigated by dynamic light scattering. It was the first time to observe a thermoreversible appearance/annihilation of scattering speckle. This strongly suggests that not only chemical gels but also physical gels have frozen inhomogeneities. Decomposition of the scattered intensity to those from thermal concentration fluctuations, $\langle I_F \rangle_T$, and static inhomogeneities, was successfully carried out with the same manner employed for chemical gels. It was found that $\langle I_F \rangle_T$ is rather temperature independent and the speckle is solely due to the static inhomogeneities. We believe that physical gels have many common features with glasses and the glassy inhomogeneities in gels will give rise to such universality as has been found in glass-forming systems.

[1] P. N. Pusey and W. van Megen, Physica (Amsterdam) **157A**, 705 (1989).
[2] J. Bastide and L. Leibler, Macromolecules **21**, 2647 (1988).
[3] S. Panyukov and Y. Rabin, Macromolecules **29**, 7960 (1996).
[4] S. Panyukov and Y. Rabin, Phys. Rep. **269**, 1 (1996).
[5] A. Onuki, J. Phys. II (France) **2**, 45 (1992).
[6] Y. Shiwa, Eur. Phys. J. **B1**, 345 (1998).
[7] M. Shibayama et al., Macromolecules **27**, 1738 (1994).
[8] M. Shibayama, F. Ikkai, and S. Nomura, Macromolecules **27**, 6383 (1994).
[9] J. E. Martin, J. Wilcoxon, and J. Odinek, Phys. Rev. A **43**, 858 (1991).
[10] P. Lang and W. Burchard, Macromolecules **24**, 814 (1991).
[11] S. Z. Ren and C. M. Sorensen, Phys. Rev. Lett. **70**, 1727 (1993).
[12] A. Onuki, Non-Cryst. Solids **172–174**, 1151 (1994).
[13] M. Shibayama and T. Norisuye, in *Proceedings of the 8th Tohwa University International Symposium on Slow Dynamics in Complexed Systems* (AIP, Fukuoka, Japan, 1998), p. 85.
[14] G. P. Johari and M. Goldstein, J. Chem. Phys. **53**, 2372 (1970).
[15] D. Stauffer, *Introduction to Percolation Theory* (Taylor & Francis, London, 1985).
[16] M. Adam and D. Lairez, in *Physical Properties of Polymeric Gels,* edited by J. P. Cohen Addad (John Wiley & Sons, New York, 1996), p. 87.
[17] T. Tanaka, L. O. Hocker, and G. B. Benedek, J. Chem. Phys. **59**, 5151 (1973).
[18] M. Shibayama, Macromol. Chem. Phys. **199**, 1 (1998).
[19] J. G. H. Joosten, J. L. McCarthy, and P. N. Pusey, Macromolecules **24**, 6690 (1991).
[20] F. Horkay et al., Macromolecules **26**, 3375 (1993).
[21] M. Shibayama, Y. Fujikawa, and S. Nomura, Macromolecules **29**, 6535 (1996).
[22] M. Shibayama, T. Norisuye, and S. Nomura, Macromolecules **29**, 8746 (1996).
[23] T. Norisuye, M. Takeda, and M. Shibayama, Macromolecules **31**, 5316 (1998).
[24] W. Goetze and L. Sjogren, Prog. Rep. Phys. **55**, 241 (1992).